JVST A
Journal of Vacuum Science & Technology A

Temperature dependence of on–off ratio and reverse recovery time in NiO/β-Ga_2O_3 heterojunction rectifiers

Cite as: J. Vac. Sci. Technol. A **40**, 063407 (2022); https://doi.org/10.1116/6.0002186
Submitted: 29 August 2022 • Accepted: 17 October 2022 • Published Online: 04 November 2022

Jian-Sian Li, Chao-Ching Chiang, Xinyi Xia, et al.

JVST A
Journal of Vacuum Science & Technology A
ARTICLE
avs.scitation.org/journal/jva

Temperature dependence of on–off ratio and reverse recovery time in NiO/β-Ga_2O_3 heterojunction rectifiers

Cite as: J. Vac. Sci. Technol. A **40**, 063407 (2022); doi: 10.1116/6.0002186
Submitted: 29 August 2022 · Accepted: 17 October 2022 ·
Published Online: 4 November 2022

View Online Export Citation CrossMark

Jian-Sian Li,[1] Chao-Ching Chiang,[1] Xinyi Xia,[1] Fan Ren,[1] and S. J. Pearton[2,a)]

AFFILIATIONS

[1]Department of Chemical Engineering, University of Florida, Gainesville, Florida 32606
[2]Department of Materials Science and Engineering, University of Florida, Gainesville, Florida 32606

[a)]**Electronic mail:** spear@mse.ufl.edu

ABSTRACT

The temperature-dependent behavior of on/off ratio and reverse recovery time in vertical heterojunction p-NiO/β n-Ga_2O/n^+ Ga_2O_3 rectifiers was investigated over the temperature range of 25–300 °C. The device characteristics in forward bias showed evidence of multiple current transport mechanisms and were found to be dependent on the applied bias voltages and temperatures. The on–off ratio decreased from 3×10^6 at 25 °C to 2.5×10^4 at 300 °C for switching to 100 V reverse bias. For 200 μm diameter rectifiers, the reverse recovery time of ~21 ns was independent of temperature, with the I_{rr} monotonically increasing from 15.1 mA at 25 °C to 25.6 mA at 250 °C and dropping at 300 °C. The dI/dt increased from 4.2 to 4.6 A/μs over this temperature range. The turn-on voltage decreased from 2.9 V at 25 °C to 1.7 V at 300 °C. The temperature coefficient of breakdown voltage was negative and does not support the presence of avalanche breakdown in NiO/β-Ga_2O_3 rectifiers. The energy loss during switching from 100 V was in the range 23–31 μJ over the temperature range investigated.

I. INTRODUCTION

There is significant interest in Ga_2O_3 based power electronics for potential applications in hybrid-electric vehicles, wireless charging, and power flow control in renewable energy systems.[1–12] One drawback for this material system is the absence of a practical p-type doping capability,[13–19] but progress has been made in heterojunction devices involving using a heterojunction of $(AlxGa_{1-x})_2O_3/Ga_2O_3$ (Ref. 2) or p-type oxides, especially NiO.[20–33] There is still a need to fully understand the high on-resistance (R_{on}) and switching characteristics of conventional Schottky rectifiers and heterojunction rectifiers.[34–40]

For Schottky contacts on Ga_2O_3, there is now a fairly good framework to understand their behavior.[41–51] The highest reported barrier height values of ~2.1 eV have been reported for oxidized metal contacts of PtO_x and IrO_x deposited by reactive sputtering on (−201) Ga_2O_3 substrates.[47] Extending this to the use of p-type metal oxides allows a transition to p–n junction behavior and also the incorporation of the oxide in edge termination schemes.[20–33,52]

In this paper, we report on the temperature dependence of switching characteristics of vertical heterojunction p-NiO/β n-Ga_2O/n^+ Ga_2O_3 rectifiers, in which the NiO is deposited by sputtering and the p-type carrier concentration can be controlled by the gas ratios during deposition.

II. EXPERIMENT

The device structure was a 10 μm thick epitaxial layer (2×10^{16} cm^{-3}) grown by halide vapor phase epitaxy (HVPE) on a (001) surface orientation n^+ β-Ga_2O_3 single crystal substrate (Novel Crystal Technology, Japan). The backside Ti/Au Ohmic contact was deposited by e-beam evaporation and annealed at 550°C for 60 s under N_2.[36,53] The frontside NiO was deposited by magnetron sputtering (3 mTorr, 150 W, 13.56 MHz) from two targets to achieve a deposition rate of ~0.2 Å s^{-1}. The carrier concentration in the bilayer (10/10 nm) structure was controlled by the Ar/O_2 ratio during sputtering at levels of 2×10^{18}–3×10^{19} cm^{-3}, with mobility < 1 cm^2 V^{-1} s^{-1}. This structure was to optimize both breakdown voltage and contact resistance.[50] Ni/Au contact metal (200–1000 μm diameter) was deposited onto the NiO layer after annealing at 300 °C under O_2 ambient. Figure 1 shows both

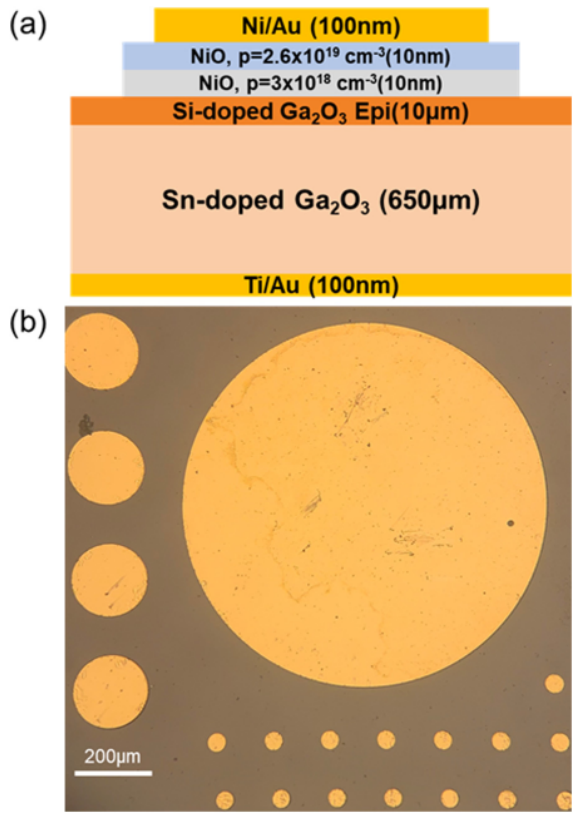

FIG. 1. (a) Schematic of the optimized NiO/Ga_2O_3 heterojunction rectifier. (b) Optical microscope image of completed device.

(a) schematic of the device structure and (b) optical image of the completed device.

The current–voltage (*I*–*V*) characteristics were recorded with a Tektronix 370-A curve tracer, 371-B curve tracer and Agilent 4156C was used for forward and reverse current measurements over the temperature range of 25–300 °C. The reverse recovery was measured on a pulse generator at low bias (10 V), while the power loss during switching was also measured at higher voltage (100 V) using an inductive-load circuit.[17]

III. RESULTS AND DISCUSSION

Figure 2 shows the temperature-dependent forward current density–voltage (*J*–*V*) characteristics of the heterojunction rectifiers, as well as the differential specific on-resistance (R_{on}) values, which at 25 °C was 14.2 mΩ cm^2. Different regions with obvious inflection points can be observed before the effect of series resistance dominates beyond 2.5 V, implying the existence of multiple current conduction mechanisms. This is different from a conventional Schottky rectifier, which generally only shows two regions in which the current at low forward voltages (<0.5 V) is dominated by tunneling, while between 0.5 and 1 V, follows an exponential relation

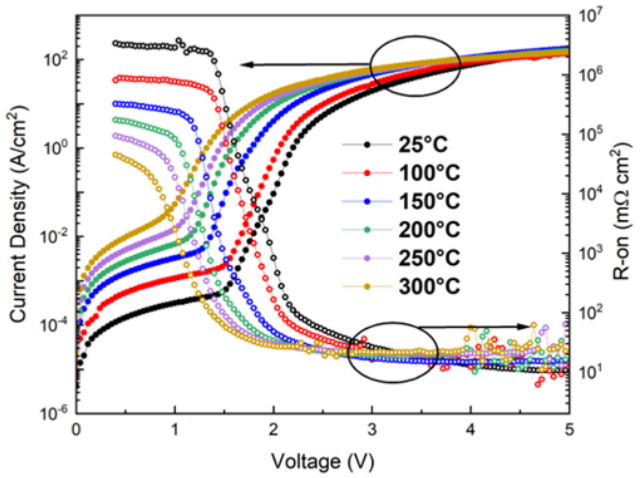

FIG. 2. Temperature dependence of forward current density and on-state resistance.

due to recombination-tunneling. The forward current in the heterojunctions is most likely dominated by hole injection from the p-NiO to n-Ga_2O_3. Previous reports have ascribed the different regions to tunneling at low bias, diffusion conduction at moderate forward bias, and space-charge-limited current prior to the effect of series resistance.[39,54] The R_{on} values show a reduction with increasing forward bias, possibly from conductivity modulation from hole injection. The devices showed excellent rectification characteristics over the entire temperature range.

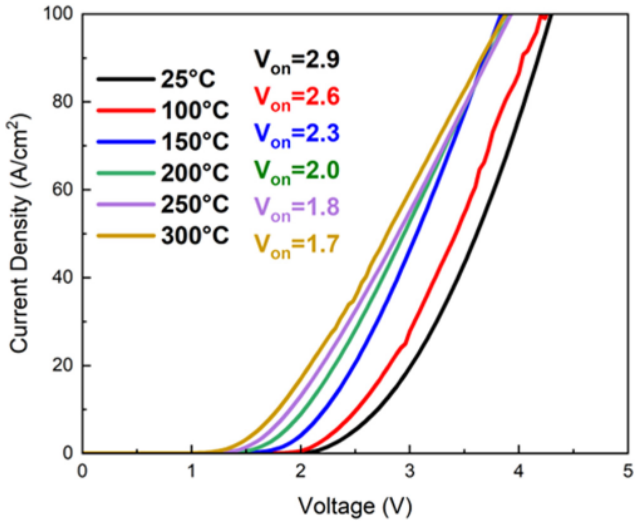

FIG. 3. Temperature dependence of forward turn-on voltage. The voltage shifts to lower values with increasing temperature.

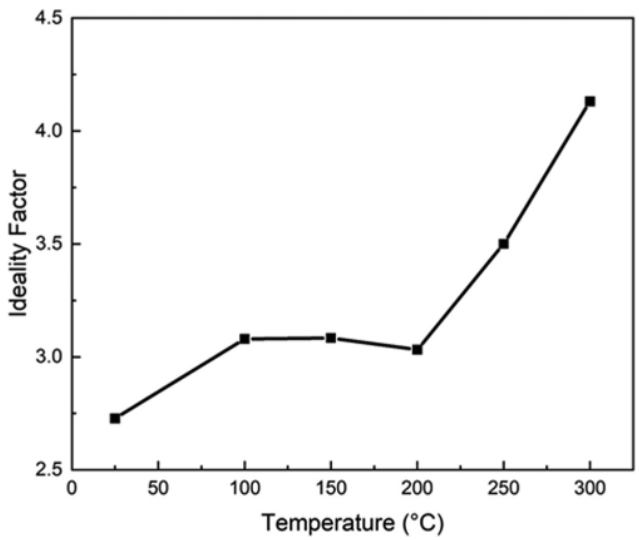

FIG. 4. Ideality factor as a function of temperature, derived from plots of ln (I) vs V.

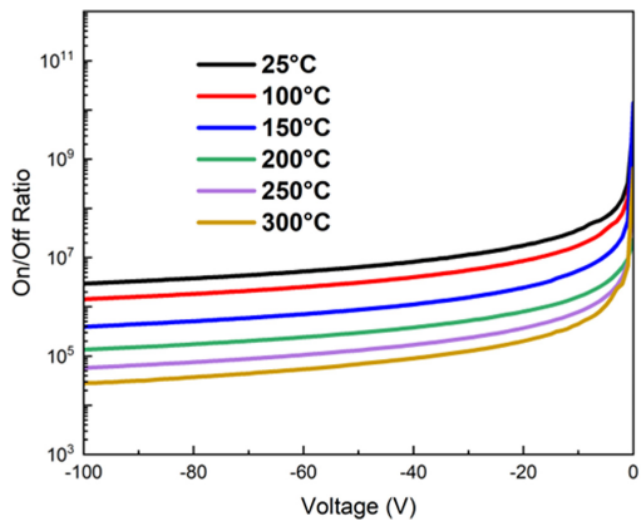

FIG. 6. Temperature dependence of on–off ratio when switching from −10 V forward to the reverse voltage shown on the *x* axis. This ratio decreases with increasing temperature.

Figure 3 shows the turn-on voltage (Von, extracted by linear fitting the forward region) was approximately 2.9 V at room temperature and decreased monotonically with temperature. The turn-on voltage is larger than that of the conventional Schottky rectifier on the same device structure. The NiO/Ga_2O_3 heterojunction band alignment is a type-II staggered configuration, in which the valence/conduction bands of the NiO are approximately 0.9/0.2 eV higher than that of Ga_2O_3,[52] respectively. Therefore, under forward bias, there is upward bending of the conduction band of Ga_2O_3 at the interface with NiO and the conduction band offset is sufficient to accumulate electrons at the Ga_2O_3, while holes in the valence band of the NiO are injected into the Ga_2O_3 at low bias voltage. The shift of turn-on voltage with temperature is due to the decrease in the barrier width due to diffusion of holes.

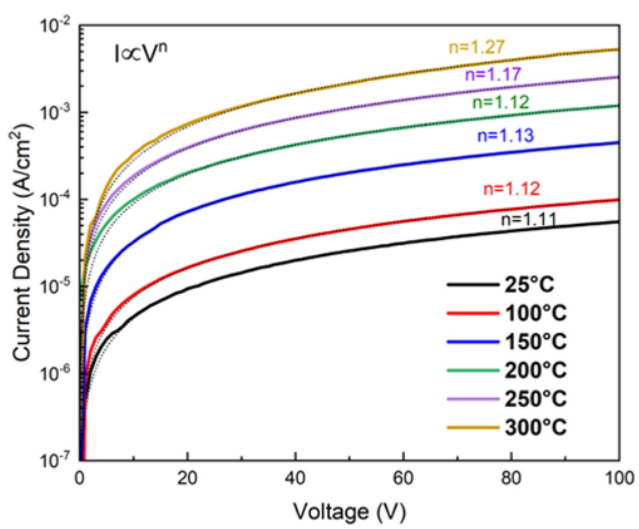

FIG. 5. Temperature dependence of reverse current density in NiO/Ga_2O_3 rectifiers. Current increases with temperature.

The ideality factor, *n*, values at different temperatures were obtained from the slope of the ln *I*–*V* plot and were in the range ~2.5–4, as shown in Fig. 4. These values >1 suggest the presence of defect states in the NiO. The activation energy (ΔE) was ~0.75 eV for the heterojunction. There are several trap states reported at this energy for β-Ga_2O_3, but the origin is not yet clear.[53] In addition, the recombination-tunneling current transport was suppressed at higher temperature, suggesting diffusion conduction is dominant.

The reverse *I*–*V* characteristics of the heterojunction diodes are shown in Fig. 5 and were fitted to the usual pn junction

TABLE I. Summary of switching performance of heterojunction NiO/Ga_2O_3 rectifiers without circuit board.

T (°C)	T_{rr} (ns)	I_{rr} (mA)	dI/dt (A μs)	I_F (mA)	Energy loss (nJ)
25	21	−15	4.2	80	27
100	22	−17	4.3	80	28
150	21	−20	4.4	80	29
200	22	−22	4.5	80	30
250	21	−26	4.6	80	34
300	21	−21	4.6	80	34

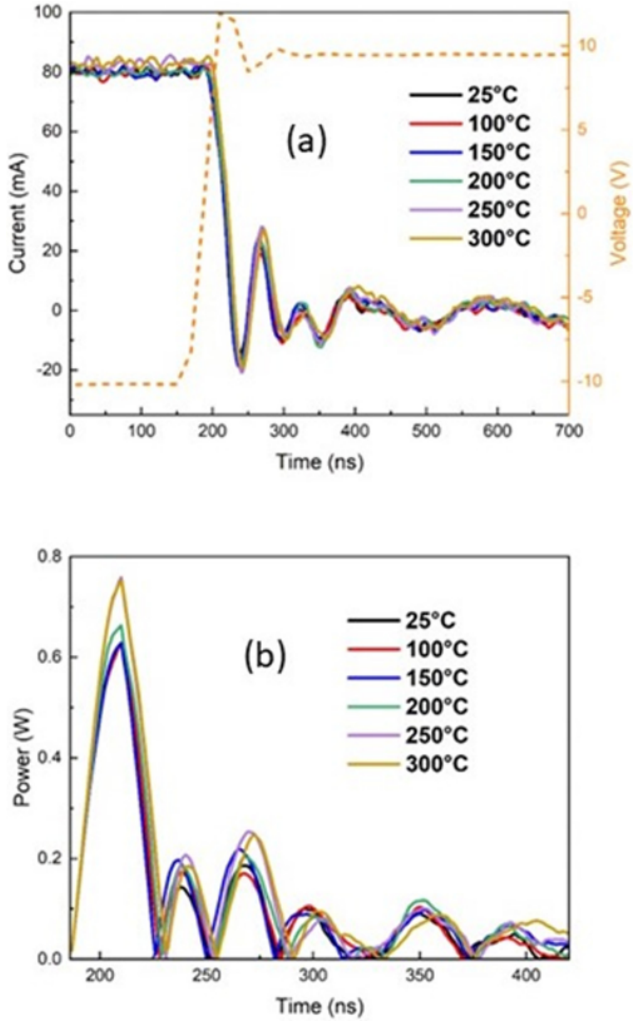

FIG. 7. Temperature dependence of (a) switching characteristics and (b) power loss of vertical rectifiers under pulsed conditions (period = 50 μs, duty cycle = 1 μs (20%), power supply = ± 10 V) without circuit board.

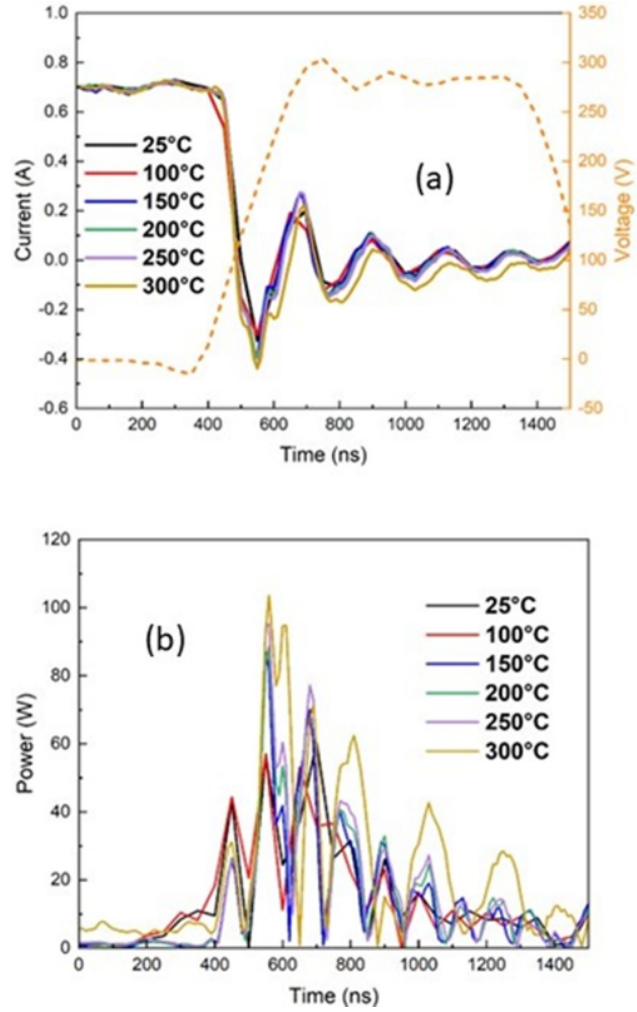

FIG. 8. Temperature dependence of (a) switching characteristics and (b) power loss of vertical rectifiers under pulsed conditions (period = 50 μs, duty cycle = 0.1 μs (2%), voltage switched from 100 V) with circuit board.

equation. The breakdown voltage showed a negative temperature coefficient, showing that impact ionization is not the breakdown mechanism since that should exhibit positive temperature coefficient.[1,3,6] The absolute breakdown voltage is lower than the theoretical value because of the presence of defects in the starting substrate and epi layers, as is typical for new technologies and is widely reported or Ga_2O_3.[7,8] At lower voltages, reverse bias leakage current was dominated by thermionic field emission (TFE). The leakage current showed a good fit to the TFE model when the reverse voltage was less than 50 V. At higher voltages, electron injection into the drift region produces an $I \propto V^n$ relationship with the voltage, indicating trap-assisted space-charge-limited conduction (SCLC). The reverse current characteristics at different temperatures all show a $I \propto V^n$, with $n < 2$. Values of >2 would be obtained if trap charge-limited SCLC with an exponent distribution of traps was dominant.

The on–off ratio is another figure of merit in that having high on-current and low leakage current in reverse bias is desirable. This was $>10^5$ for all temperatures measured, as shown in Fig. 6, but decreased with increasing temperature due to an increase in reverse current.

The reverse recovery time of ~21 ns was independent of temperature, with the I_{rr} monotonically increasing from 15.1 mA at 25 °C to 25.6 mA at 250 °C. The dI/dt increased from 4.2 to 4.6 A μs over this temperature range, as summarized in Table I. The reverse recovery time is defined as the time required to reach

TABLE II. Summary of switching performance of heterojunction NiO/Ga_2O_3 rectifiers with circuit board.

T (°C)	T_{rr} (ns)	I_{rr} (mA)	dI/dt (A μs)	I_F (A)	Energy loss (μJ)
25	102	−0.3	12.6	0.7	23.1
100	104	−0.3	13.8	0.7	24.1
150	117	−0.4	19.8	0.7	24.3
200	123	−0.4	19.8	0.7	25.6
250	127	−0.4	20.7	0.7	26.5
300	144	−0.4	21.8	0.7	31.3

25% of the peak current. As can be seen in Fig. 7(a), the reverse recovery time is basically independent of temperature. The switching loss is plotted in Fig 7(b). These were measured at relatively low voltage so that we did not need the inductive-load switching circuit that allows higher biases, but whose power transistors dominate reverse recovery times.[17] Lu *et al.*[55] reported 14 ns for similar Schottky rectifiers. Our values for the NiO/Ga_2O_3 are roughly twice this result. Gong *et al.*[30,31] reported a reverse recovery time of 11 ns on a NiO/Ga_2O_3 heterojunction rectifier of 1 mm^2 area, although this was defined as recovery of current to 10% of its peak value, whereas other reports use 25%. Though the changes were small, we found in general that the peak reverse recovery current increased with increasing dI/ dt, and the recovery time decreased with increasing dI/dt.

Finally, we measured the switching waveform and turn-off power loss for 1 mm diameter devices, as shown in Figs. 8(a) and 8(b), respectively, for switching from 100 V within the inductive-load circuit. Note that under these conditions, the reverse recovery time is dominated by the Si power MOSFET in the measuring circuit, leading to a measurement-limited value >100 ns (Table II), but the turn-off power loss is accurate and gives some indication of switching performance under more practical voltages and currents. The magnitude of reverse recovery current produced by the NiO/Ga_2O_3 rectifier and the peak switching power during reverse recovery is significantly lower as compared to typical Si ultrafast diodes, indicating these heterojunction rectifiers are applicable to high power and high frequency applications.

IV. SUMMARY AND CONCLUSIONS

Vertical p-NiO/ n-Ga_2O_3 heterojunction rectifiers show turn-on voltage and specific on-resistance of <2.9 V over temperatures of up to 300 °C. The turn-on voltage decreased with temperature, while the on-state resistance increased. The on–off ratio decreased from 3×10^6 at 25 °C to 2.5×10^4 at 300 °C for switching to 100 V reverse bias. For 200 μm diameter rectifiers, the reverse recovery was independent of temperature, suggesting the excellent potential of these devices for elevated temperature power switching.

ACKNOWLEDGMENTS

The work at UF was performed as part of Interaction of Ionizing Radiation with Matter University Research Alliance (IIRM-URA), sponsored by the Department of the Defense, Defense Threat Reduction Agency under Award No. HDTRA1-20-2-0002. The content of the information does not necessarily reflect the position or the policy of the federal government, and no official endorsement should be inferred. The work at UF was also supported by NSF DMR 1856662 (James Edgar).

AUTHOR DECLARATIONS

Conflict of Interest

The authors have no conflicts to disclose.

Author Contributions

Jian-Sian Li: Data curation (equal); Formal analysis (equal); Investigation (equal); Methodology (equal); Writing – original draft (equal). **Chao-Ching Chiang:** Data curation (equal); Formal analysis (equal); Investigation (equal). **Xinyi Xia:** Data curation (equal); Formal analysis (equal); Investigation (equal). **Fan Ren:** Conceptualization (equal); Data curation (equal); Formal analysis (equal); Funding acquisition (equal); Investigation (equal); Writing – original draft (equal). **S. J. Pearton:** Conceptualization (equal); Supervision (equal); Writing – original draft (equal).

DATA AVAILABILITY

The data that support the findings of this study are available within the article.

REFERENCES

[1] J. Ballestín-Fuertes, J. Muñoz-Cruzado-Alba, J. F. Sanz-Osorio, and E. Laporta-Puyal, Electronics **10**, 677 (2021).
[2] Prakash P. Sundaram, Fikadu Alema, Andrei Osinsky, and Steven J. Koester, J. Vac. Sci Technol. A **40**, 043211 (2022).
[3] J. Y. Tsao *et al.*, Adv. Electron. Mater. **4**, 1600501 (2018).
[4] Y. Sun *et al.*, Electronics **8**, 575 (2019).
[5] M. H. Wong and M. Higashiwaki, IEEE Trans. Electron. Devices **67**, 3925 (2020).
[6] Andrew J. Green *et al.*, APL Mater. **10**, 029201 (2022).
[7] S. J. Pearton, Fan Ren, Marko Tadjer, and Jihyun Kim, J. Appl. Phys. **124**, 220901 (2018).
[8] S. Sharma, K. Zeng, S. Saha, and U. Singisetti, IEEE Electron. Device Lett. **41**, 836 (2020).
[9] Jiancheng Yang, F. Ren, Marko Tadjer, S. J. Pearton, and A. Kuramata, AIP Adv. **8**, 055026 (2018).
[10] S. Roy, A. Bhattacharyya, P. Ranga, H. Splawn, J. Leach, and S. Krishnamoorthy, IEEE Electron. Device Lett. **42**, 1140 (2021).
[11] W. Li, K. Nomoto, Z. Hu, D. Jena, and H. G. Xing, IEEE Electron. Device Lett. **41**, 107 (2020).
[12] Ribhu Sharma, Minghan Xian, Chaker Fares, Mark E. Law, Marko Tadjer, Karl D. Hobart, Fan Ren, and Stephen J. Pearton, J. Vac. Sci. Technol. A **39**, 013406 (2021).
[13] Wenshen Li, Devansh Saraswat, Yaoyao Long, Kazuki Nomoto, Debdeep Jena, and Huili Grace Xing, Appl. Phys. Lett. **116**, 192101 (2020).
[14] Y. Lv *et al.*, IEEE Trans. Power Electron. **36**, 6179 (2021).
[15] Jiancheng Yang *et al.*, Appl. Phys. Lett. **114**, 232106 (2019).
[16] Z. Jian, S. Mohanty, and E. Ahmadi, Appl. Phys. Lett. **116**, 152104 (2020).
[17] J. Yang, F. Ren, Y.-T. Chen, Y.-T. Liao, C.-W. Chang, J. Lin, M. J. Tadjer, S. J. Pearton, and A. Kuramata, IEEE J. Electron. Devices **7**, 57 (2019).
[18] T. Harada and A. Tsukazaki, Appl. Phys. Lett. **116**, 232104 (2020).
[19] C.-H. Lin *et al.*, IEEE Electron. Device Lett. **40**, 1487 (2019).

[20]W. Xiong *et al.*, IEEE Electron. Device Lett. **42**, 430 (2021).
[21]S. J. Pearton, J. Yang, P. H. Cary, F. Ren, J. Kim, M. J. Tadjer, and M. A. Mastro, Appl. Phys. Rev. **5**, 011301 (2018).
[22]Ming Xiao *et al.*, IEEE Trans. Power Electron. **36**, 8565 (2021).
[23]Arkka Bhattacharyya *et al.*, Appl. Phys. Express **15**, 061001 (2022).
[24]X. Lu, Xianda Zhou, Huaxing Jiang, Kar Wei Ng, Zimin Chen, Yanli Pei, Kei May Lau, and Gang Wang, IEEE Electron. Device Lett. **41**, 449 (2020).
[25]Chenlu Wang *et al.*, IEEE Electron. Device Lett. **42**, 485 (2021).
[26]S. Roy, A. Bhattacharyya, P. Ranga, H. Splawn, J. Leach, and S. Krishnamoorthy, IEEE Electron. Device Lett. **42**, 1540 (2021).
[27]Qinglong Yan *et al.*, Appl. Phys. Lett. **118**, 122102 (2021).
[28]H. H. Gong, X. H. Chen, Y. Xu, F.-F. Ren, S. L. Gu, and J. D. Ye, Appl. Phys. Lett. **117**, 022104 (2020).
[29]Hehe Gong *et al.*, IEEE Trans. Power Electron. **36**, 12213 (2021).
[30]H. H. Gong *et al.*, Appl. Phys. Lett. **118**, 202102 (2021).
[31]H. H. Gong, X. H. Chen, Y. Xu, Y. T. Chen, F. F. Ren, B. Liu, S. L. Gu, R. Zhang, and J. D. Ye, IEEE Trans. Electron. Devices **67**, 3341 (2020).
[32]W. Hao *et al.*, Appl. Phys. Lett. **118**, 043501 (2021).
[33]F. Zhou *et al.*, IEEE Trans. Power Electron. **37**, 1223 (2022).
[34]Qinglong Yan *et al.*, Appl. Phys. Lett. **120**, 092106 (2022).
[35]*Gallium Oxide Vertical Transistor with the World's Highest Breakdown Voltage* (Novel Crystal Technology, Tokyo, 2021), see https://www.novelcrystal.co.jp/eng/2021/911/
[36]Jiancheng Yang, Fan Ren, Marko Tadjer, S. J. Pearton, and A. Kuramata, ECS J. Solid State Sci. Technol. **7**, Q92 (2018).
[37]Pengfei Dong, Jincheng Zhang, Qinglong Yan, Zhihong Liu, Peijun Ma, Hong Zhou, and Yue Hao, IEEE Electron. Device Lett. **43**, 765 (2022).
[38]J. A. Spencer, A. L. Mock, A. G. Jacobs, M. Schubert, Y. Zhang, and M. J. Tadjer, Appl. Phys. Rev. **9**, 011315 (2022).
[39]Yuangang Wang *et al.*, IEEE Trans. Power Electron. **37**, 3743 (2022).
[40]W. Li, D. Jena, and H. G. Xing, J. Appl. Phys. **131**, 015702 (2022).
[41]Hardhyan Sheoran, Vikram Kumar, and Rajendra Singh, ACS Appl. Electron. Mater. **4**, 2589 (2022).
[42]Lisa M. Porter and Jenifer R. Hajzus, J. Vac. Sci. Technol. A **38**, 031005 (2020).
[43]Xinyi Xia, Minghan Xian, Chaker Fares, Fan Ren, Marko Tadjer, and Stephen J. Pearton, J. Vac. Sci. Technol. A **39**, 053405 (2021).
[44]Minghan Xian, Chaker Fares, Fan Ren, Brent P. Gila, Yen-Ting Chen, Yu-Te Liao, Marko Tadjer, and Stephen J. Pearton, J. Vac. Sci. Technol. B **37**, 061201 (2019).
[45]Ming-Hsun Lee and Rebecca L. Peterson, J. Mater. Res. **36**, 4771 (2021).
[46]Ming-Hsun Lee, Ta-Shun Chou, S. Bin Anooz, Zbigniew Galazka, Andreas Popp, and Rebecca L. Peterson, ACS Nano **1**, 11988 (2022).
[47]Caixia Hou, Rodrigo M. Gazoni, Roger J. Reeves, and Martin W. Allen, IEEE Trans. Electron. Devices **68**, 1791 (2021).
[48]E. Farzana, Z. Zhang, P. K. Paul, A. R. Arehart, and S. A. Ringel, Appl. Phys. Lett. **110**, 202102 (2017).
[49]C. Fares, F. Ren, and S. J. Pearton, ECS J. Solid State Sci. Technol. **8**, Q3007 (2019).
[50]Jian-Sian Li, Chao-Ching Chiang, Xinyi Xia, Fan Ren, Honggyu Kim, and S. J. Pearton, Appl. Phys. Lett. **121**, 042105 (2022).
[51]Yen-Ting Chen, Jiancheng Yang, Fan Ren, Chin-Wei Chang, Jenshan Lin, S. J. Pearton, Marko J. Tadjer, Akito Kuramata, and Yu-Te Liao, ECS J. Solid State Sci. Technol. **8**, Q3229 (2019).
[52]Xinyi Xia, Jian Sian Li, Chao Ching Chiang, Timothy Jinsoo Yoo, Fan Ren, Honggyu Kim, and S. J. Pearton, J. Phys. D: Appl. Phys. **55**, 385105 (2022).
[53]Xinyi Xia, Jian Sian Li, Chao Ching Chiang, Timothy Jinsoo Yoo, Fan Ren, Honggyu Kim, and S. J. Pearton, J. Vac. Sci. Technol. A **40**, 053401 (2022).
[54]Alexander Y. Polyakov, Vladimir I. Nikolaev, Eugene B. Yakimov, Fan Ren, Stephen J. Pearton, and Jihyun Kim, J. Vac. Sci. Technol. A **40**, 020804 (2022).
[55]Xing Lu, Xu Zhang, Huaxing Jiang, Xinbo Zou, Kei May Lau, and Gang Wang, Phys. Status Solidi A **217**, 1900497 (2020).